Sustainable Food Technology

ROYAL SOCIETY OF CHEMISTRY

PAPER

View Article Online
View Journal | View Issue

Cite this: *Sustainable Food Technol.*, 2025, **3**, 2282

Investigation of polymer blend formulation and homogenization dynamics in the development of biodegradable, hydrophobic, and heat-resistant seaweed-based bioplastic straws

Wahyu Ramadhan, †[ab] Joko Santoso,†[a] Uju, *[ac] Rahadiyan Garuda Langit Dewangga,[d] Mario Natanael,[a] Muhammad Aldy Luthfiansyah,[a] Adinda Yulya Rachmawati[ad] and Zacky Arivaie Santosa[a]

The demand for biodegradable straws has grown in response to environmental concerns regarding plastic waste. This study aimed to develop and optimize seaweed-based bioplastic straws with enhanced hydrophobicity, mechanical integrity, and biodegradability. Four base formulations combining agar, starch, carrageenan, and konjac were evaluated, with the B9 formulation (comprising agar and starch) selected as the most promising due to its superior thermal stability and low water absorption. This formulation was then used in a process optimization stage, where various homogenization parameters (speed, temperature, and time) were tested. The best-performing straw from this stage, referred to as low-speed-S-B9 (B9 processed under low-speed homogenization), demonstrated the most favorable overall performance, achieving a contact angle of 115.31 ± 1.15°, water absorption below 100.27 ± 2.67%, and tensile strength of 60.76 ± 2.78 MPa. SEM analysis revealed a dense and cohesive matrix structure, while FTIR spectra showed the main polysaccharide functional groups in all samples, with additional peaks reflecting each formulation's chemical composition. Thermal degradation profiles confirmed its heat resistance, with delayed onset and higher char residue. Mechanical and flexural tests showed the low-speed straw maintained high elongation and comparable bending resistance to commercial paper straws. Finally, soil burial testing confirmed full biodegradation of the straw within 60 days. These results confirm that low-speed homogenization of seaweed-based formulations offers a scalable and sustainable strategy to produce biodegradable straws with functional properties suitable for real-world use.

Received 1st July 2025
Accepted 2nd October 2025

DOI: 10.1039/d5fb00344j

rsc.li/susfoodtech

Sustainability spotlight

Our research directly supports multiple United Nations Sustainable Development Goals (SDGs), particularly SDG 12 (Responsible Consumption and Production) and SDG 14 (Life Below Water). By valorizing seaweed—a renewable marine biomass—as the primary resource for bioplastic straws, we contribute to reducing reliance on fossil-based plastics and mitigating ocean plastic pollution, a critical threat to marine biodiversity. Furthermore, the development of biodegradable, thermally stable, and hydrophobic straws promotes sustainable material innovation for food-contact applications, minimizing waste and enhancing lifecycle sustainability. The use of low-speed homogenization for straw processing also supports SDG 9 (Industry, Innovation and Infrastructure) by offering an energy-efficient and scalable manufacturing route. Overall, this work integrates circular economy principles and marine biomass valorization, advancing environmentally responsible food packaging systems aligned with the global sustainability agenda.

1 Introduction

Plastic pollution has emerged as a pressing global environmental crisis, threatening ecosystems, biodiversity, and human health through microplastic contamination, degradation of marine habitats, and the long-term accumulation of non-biodegradable waste in landfills.[1–4] Global plastic production increased from 353 million metric tons in 2019 to more than 400 million tons in 2022, with projections exceeding 1 billion metric tons annually by 2060 if current practices persist.[5,6]

[a]*Department of Aquatic Product Technology, Faculty of Fisheries and Marine Sciences, IPB University, Bogor 16680, Indonesia. E-mail: ujusadi@apps.ipb.ac.id*

[b]*Center of Coastal and Marine Resources Studies (PKSPL), International Research Institute for Maritime, Ocean and Fisheries (i-MAR), IPB University, Bogor 16127, Indonesia*

[c]*Surfactant and Bioenergy Research Center (SBRC), IPB University, Bogor 16127, Indonesia*

[d]*PT IJO Inovasi Indonesia, Jl. Ciledug Raya No.125 B, Cipulir, Kebayoran Lama, Jakarta 12230, Indonesia*

† WR and JS equally contributed to this work and share common first authorship.

Single-use plastic straws, widely used and rapidly discarded, are a visible contributor to this problem. Although paper straws have been introduced as an alternative, their poor wet resistance, limited mechanical strength, and low user acceptance restrict their effectiveness as a sustainable replacement. These shortcomings, together with the increasing scale of plastic waste, underscore the urgent need for more durable and environmentally sustainable alternatives.

In response to this escalating crisis, governments and regulatory bodies worldwide have introduced stringent measures aimed at reducing plastic consumption through bans, financial incentives, and mandates for sustainable product design. This regulatory landscape, coupled with increased consumer awareness, has accelerated research into biodegradable and renewable alternatives that can effectively replace conventional plastics without sacrificing essential performance attributes.[7–12] Among these products, disposable drinking straws, typically fabricated from polypropylene or polystyrene, have become a focal point due to their extensive usage, short lifecycle, and prominent role in environmental degradation.

Bioplastics derived from biomass such as cellulose, gelatin, and starch have attracted considerable interest. However, their widespread adoption remains hindered by critical limitations, notably poor thermal resistance, insufficient mechanical integrity, and high water affinity, which restrict their applicability, particularly in high-temperature, food-contact scenarios.[13–15] Consequently, attention has increasingly shifted toward marine-derived biomass, particularly seaweed-based polysaccharides, as sustainable and scalable sources of high-performance biopolymer.[16–19] Seaweeds like *Gelidium* and *Gracilaria* are especially promising owing to their rapid growth rates, high polysaccharide yields, and their inherent capability for atmospheric carbon sequestration during cultivation, making them strategically advantageous from both environmental and industrial perspectives.[20,21] Moreover, the global movement towards utilizing seaweed-based polymers is gaining momentum due to their unique ability to significantly increase biomass productivity without requiring additional arable land or freshwater resources, thus avoiding competition with essential human food and agricultural needs.

Despite their sustainability credentials, seaweed-based biopolymers, particularly agar-based films, exhibit several performance deficits that critically limit their broader industrial and consumer acceptance. Agar films are inherently hydrophilic, possess inadequate mechanical strength, and exhibit limited thermal stability, thus constraining their practical use in applications that involve prolonged moisture exposure or elevated temperatures.[22,23] Addressing these deficits necessitates innovative formulation strategies to enhance their functional properties while maintaining biodegradability and ensuring industrial scalability.

Polymer blending has been widely adopted as a strategic method to overcome natural limitations of single-component biopolymers. The integration of agar with other polysaccharides, such as carrageenan[24,25] and corn starch,[26,27] along with natural hydrophobic substances like beeswax,[28] has been demonstrated to synergistically enhance mechanical integrity, thermal stability, and hydrophobicity. Additionally, the inclusion of inorganic fillers such as calcium carbonate ($CaCO_3$) provides improved mechanical reinforcement and stability under thermal stress.[29,30] Such composite approaches are essential for tailoring the physicochemical properties necessary to render seaweed-based bioplastic materials suitable for practical applications, particularly for food-contact packaging such as drinking straws. However, although various additives have been incorporated into agar-based matrices in previous studies, none has integrated all these components within a single formulation to comprehensively enhance performance, particularly in improving the hydrophobicity, heat resistance, and durability of agar-based biodegradable drinking straws.

Beyond compositional factors, the manufacturing process significantly influences the microstructural characteristics and resultant properties of bioplastics. Specifically, homogenization techniques, including mixing speed, temperature, and duration, critically determine the dispersion quality, interfacial adhesion, and morphological uniformity within polymer blends.[14,31,32] Technically, high-shear homogenization (>10 000 rpm) has been the method of choice due to its effectiveness in achieving homogeneous dispersion at laboratory scale. However, its high energy consumption, scalability constraints, and operational complexity limit its practicality for industrial production. Conversely, low-speed homogenization methods (<10 000 rpm), such as overhead stirring, offer viable industrial alternatives with reduced energy demands and greater scalability potential, though their effectiveness in maintaining or enhancing bioplastic performance remains underexplored.

To bridge these critical gaps, this study systematically investigates the integrated effects of polymer blend composition and low-speed homogenization conditions on the development of biodegradable, hydrophobic, and heat-resistant seaweed-based bioplastic straws. Employing a factorial experimental design, the research evaluates the individual and combined impacts of polymer components (agar, carrageenan, corn starch, konjac, beeswax, $CaCO_3$, citric acid) and optimized processing parameters (homogenization speed, temperature, and duration) on key functional attributes including surface hydrophobicity (contact angle), tensile properties, thermal degradation behavior, water absorption, and biodegradability. The outcomes of this research are expected to advance the development of sustainable bioplastic alternatives to petroleum-derived straws, supporting industrial feasibility, and contributing meaningfully to global efforts toward circular materials economies and sustainable resource management.

2 Material and methods

2.1 Materials

Agar powder (food grade) was purchased from CV Sari Mutiara Abadi (Indonesia). κ-Carrageenan powder (food grade) was obtained from Kappa Carrageenan Nusantara, Pasuruan, Indonesia, and konjac flour (food grade) was sourced from Hubei Yizhi Konjac Biotechnology Co., Ltd, China. Corn starch (food grade, Bola Deli Maizena, Indonesia) and beeswax (Cera Alba, food grade, Shanghai, China) were used as biopolymer and

hydrophobic additives. Sorbitol (food grade; E420), calcium carbonate ($CaCO_3$, food grade; E170), and citric acid (food grade; E330) were purchased from Indo Food Chem, Jakarta, Indonesia. Distilled water was used for all solution preparations. Paper straws were utilized as a commercial standard. All chemicals used for analytical and instrumental evaluations were obtained from PT Merck Chemicals and Life Sciences (Darmstadt, Germany) and were of analytical grade unless otherwise specified.

2.2 Methods

2.2.1 Sample preparation. The bioplastic films were prepared following a modified method adapted from Rhim,[24] in which agar and κ-carrageenan are dissolved in hot water to form a casting solution. In the present work, the formulation was adjusted by incorporating konjac flour, replacing glycerol with sorbitol, and adding calcium carbonate, citric acid, and beeswax to enhance mechanical strength and water resistance. The detailed procedure is as follows: all ingredients were dissolved in 500 mL of distilled water for each formulation. The ten base film formulations (B1 to B10), as outlined in Table 1, were evaluated to identify the most water-resistant bioplastic compositions.

In the first stage, each formulation was prepared by dispersing the dry ingredients into distilled water and heating to 90–95 °C under continuous stirring. The final slurry was homogenized using a high-shear homogenizer at 20 000 rpm for 5 minutes to ensure uniform dispersion. The mixture was then poured into flat glass trays and dried in a hot air oven at 50 °C for 6–7 hours. The resulting bioplastic films were demolded and characterized for water absorption and mechanical integrity. Based on these evaluations, four top-performing formulations were selected and coded as S-B1 to S-B10.

In the second stage, the selected film formulations were adapted for straw development. The straw formulation was enhanced by incorporating calcium carbonate ($CaCO_3$), beeswax, and citric acid. Beeswax, calcium carbonate ($CaCO_3$), and citric acid were incorporated to improve hydrophobicity, mechanical strength, and thermal resistance in straw form. The formulations used for straw production (the four top-performing bioplastic formulations) were incorporated with 9 g of calcium carbonate, 10 mL of beeswax, and 0.3 g of citric acid, based on previous reports by Chong *et al.*,[33] Diyana *et al.*,[34] and modified from Yoon *et al.*.[35] The preparation process followed the same thermal and mixing protocols. Beeswax was separately melted at 65 °C before being incorporated into the hot mixture, followed by citric acid and $CaCO_3$. The final slurry was homogenized using a high-shear homogenizer at 20 000 rpm for 5 minutes to ensure uniform dispersion. The hot slurry was poured into cylindrical glass molds (2 cm inner diameter × 25 cm length) with an embedded stainless-steel rod (7 mm diameter) to form the inner cavity. Gelation was allowed at room temperature for 30 minutes before the samples were demolded and dried at 50 °C for 6 hours. The resulting straws were stored in desiccators prior to further analysis.

In the third stage, using one selected formula from stage 2, process optimization was conducted using low-speed overhead stirring as a potential alternative to high-shear mixing for industrial applications. A two-level factorial experimental design was employed, with three independent variables: temperature (60–80 °C), stirring speed (1500–2000 rpm), and mixing time (15–45 minutes). Eleven treatment combinations were executed, as presented in Tables 2 and 3. For each treatment, the same ingredient composition and casting protocol were used. Agar was first dissolved in distilled water at 90–95 °C, followed by the sequential addition of corn starch, carrageenan (if applicable), konjac (if applicable), sorbitol, beeswax (pre-melted), citric acid, and $CaCO_3$ under continuous agitation. The resulting mixture was poured into the same cylindrical molds used previously.

Among the eleven trials, the best-performing treatment, based on appearance, water resistance, and structural properties, was identified and subjected to further characterization. This optimized straw was then compared against (i) the straw

Table 2 Level and code of optimization parameters for production bioplastic straws

Parameter	Code	Low (−1)	Centre point (0)	High (+1)
Temperature (°C)	a	60	70	80
Time (minute)	b	15	30	45
Stirring speed (rpm)	c	1500	1750	2000

Table 1 Bioplastic film formulations

Treat-ments	Agar (g)	Carra-geenan (g)	Corn starch (g)	Konjac (g)	Sorbitol (g)	Water (mL)
B1	2.5	2.5	0	2.5	50	150
B2	6.0	0	0	1.5	50	150
B3	5.0	2.5	0	0	50	150
B4	2.5	2.5	5.35	2.5	50	150
B5	6.0	0	5.35	1.5	50	150
B6	5.0	2.5	5.35	0	50	150
B7	7.5	0	0	0	50	150
B8	5.0	2.5	0	0	50	150
B9	7.5	0	5.35	0	50	150
B10	5.0	2.5	5.35	1.5	50	150

Table 3 Model analysis and experimental running[a]

	Parameter		
Run	Temp.	Time	Speed
1	70 (C)	30 (C)	1750 (C)
2	70 (C)	30 (C)	1750 (C)
3	80 (H)	15 (L)	1500 (L)
4	60 (L)	15 (L)	1500 (L)
5	60 (L)	45 (H)	1500 (L)
6	70 (C)	30 (C)	1750 (C)
7	60 (L)	45 (H)	2000 (H)
8	60 (L)	15 (L)	2000 (H)
9	80 (H)	15 (L)	2000 (H)
10	80 (H)	45 (H)	2000 (H)
11	80 (H)	45 (H)	1500 (L)

[a] Information: low (L), center point (C), and high (H).

produced *via* high-shear homogenization and (ii) a commercial paper straw to evaluate the effects of mixing intensity on product performance, including biodegradability, mechanical properties, and industrial scalability.

2.2.2 Characterization of bioplastic and straws

2.2.2.1 Hot-water absorption. Hot-water absorption testing was conducted for both bioplastic film and straw samples. Bioplastic samples were cut into 25 mm × 50 mm rectangles and weighed to determine the initial mass ($m1$), while straw samples were cut to a length of 50 mm. The heat resistance of the bioplastic films and straws was evaluated through their ability to maintain structural integrity during hot-water immersion. Each sample was immersed in 200 mL of distilled water maintained at 85 °C for 30 minutes, simulating the typical thermal conditions encountered during the consumption of hot beverages in industrial or end-user applications. After immersion, samples were gently blotted dry using tissue paper and weighed again to obtain the final mass ($m2$). Water absorption was calculated using the formula:

$$\text{Hot water absorption} = \frac{m2 - m1}{m1} \times 100\%$$

2.2.2.2 Water solubility. The water solubility of straw samples was determined following the procedure of Krishnamurthy and Amritkumar[36] with modifications to reflect realistic drinking conditions. Ring segments (10 mm width) were cut from selected straw formula, oven-dried at 60 °C until constant weight, and recorded as the initial mass (W_0). Samples ($n = 3$) were immersed in 200 mL of distilled water at ambient temperature (25 ± 2 °C) for 120 min under gentle stirring (100 rpm). After 6 h immersion, the sample were collected, gently blotted, redried at 60 °C until constant weight, and reweighed (W_1). Water solubility (%, w/w) was calculated as:

$$\text{Water solubility}(\%) = \frac{W_0 - W_1}{W_0} \times 100\%$$

2.2.2.3 Fourier Transform Infrared Spectroscopy (FTIR). Functional group analysis of the bioplastic straw components was performed using Fourier Transform Infrared Spectroscopy (FTIR) with a Nicolet iS ATR iD5 (Thermo Scientific, Madison, WI, USA), employing the attenuated total reflectance (ATR) method. Spectra were collected over the range of 4000 to 400 cm^{-1}.

2.2.2.4 Contact angle. Surface wettability of the samples was assessed through contact angle measurement. A 5 μL drop of distilled water was applied at three different points on each sample surface using a contact angle meter (Nachriebe 320, CAAI 2320). The droplet profile was photographed and processed using image analysis software to determine the contact angles.

2.2.2.5 Tensile strength and elongation. Tensile strength testing was carried out using a universal testing machine. Samples were prepared in dimensions of 20 mm × 60 mm and mounted on the machine, where they were stretched at a constant rate under a predefined load. Elongation was calculated by comparing the increase in length to the initial sample length. The tensile strength (τ) was calculated using the equation:

$$\tau = \frac{16}{N} \times \frac{\text{Load}}{t \times l}$$

Note: τ = tensile strength (MPa). N = number of samples. t = sample thickness (mm). l = sample width (mm).

$$\text{Elongation}(\%) = \frac{\text{Increase in length(cm)}}{\text{Initial length(cm)}} \times 100\%$$

2.2.2.6 Bending test. Flexural behavior of the straws was assessed using a three-point bending test. Samples with a length of 10 cm were positioned across two roller supports spaced approximately 30 mm apart. A load was applied at the center using a press bar mounted on a universal testing machine (Chun Yen, LC X-30KN). The flexural strength (σ) of the hollow tubular straws was calculated using the formula:

$$\sigma_{\text{hollow}} = \frac{M \cdot \gamma}{I} = \frac{\frac{F \cdot L}{4} \cdot \gamma}{\frac{\pi\left[\left(\frac{D}{2}\right)^4 - \left(\frac{d}{2}\right)^4\right]}{4}}$$

where: M = maximum bending moment. I = moment of inertia of the cross-section. γ = distance from the centroid to the outer surface. L = span length between supports. F = applied force. D = outer diameter of straw. d = inner diameter of straw.

2.2.2.7 Thermal degradation. Thermal degradation behavior of bioplastic straws was analyzed using thermogravimetric analysis. Samples were subjected to a controlled heating program from 31 °C to 700 °C at a constant rate under a nitrogen atmosphere. Weight loss was recorded as a function of temperature to determine thermal stability and decomposition patterns.

2.2.2.8 Microstructural analysis (SEM). The surface morphology of selected straw samples were observed using scanning electron microscopy (SEM) at 2000× magnification. Samples were sputter-coated with a thin layer of gold before

imaging. SEM analysis provided insight into the homogeneity of the composite matrix, filler dispersion, and the presence of voids or cracks.

2.2.2.9 Biodegradability. Biodegradation testing was conducted by burying straw samples in open soil under natural environmental conditions (exposed to sunlight and rain). The degradation process was monitored visually and gravimetrically every 20 days over a 60-day period. Changes in structural integrity and physical appearance were recorded to evaluate the biodegradation performance.

2.2.2.10 Data analysis. Preliminary formulation screening involved analysis of ten bioplastic film formulations and the four selected straw formulations sample using a completely randomized design. Prior to one-way analysis of variance (ANOVA), data and homogeneity of variance were confirmed. Tukey's multiple range test was conducted for post-hoc analysis. The optimization and factorial study employed a 2^3 full factorial design with three center points to investigate the effects of temperature, time, and stirring speed and homogenization dynamics (Table 2). XLSTAT v.2025.1 (1428) (Addinsoft, Paris, France) was used to generate eleven randomized experimental runs (Table 3) and was employed for factorial design analysis and response surface visualization. The significance of models and interactions among variables was evaluated through ANOVA at a 95% confidence level. Comparative analysis against commercial paper straws and prior formulations utilized a randomized complete block design.

3 Results and discussion

3.1 Preliminary bioplastic film and straw formulations

3.1.1 Hot water absorption of film formulations. The hot water absorption properties of the bioplastic films formulated during the preliminary stage were significantly influenced by the composition of the polymer blends. As shown in Table 1 and Fig. 1, the presence and ratio of carrageenan, konjac flour, and corn starch played a critical role in determining the hydrophilic behavior of the films. Among the ten bioplastic formulations (B1–B10), the values of water absorption ranged from 52.73% to 217.90%. The highest absorption was observed in B4 (217.90%), which incorporated agar, konjac flour, citric acid, and $CaCO_3$. This result aligns with literature indicating that konjac, rich in glucomannan, acts as a hydrophilic fiber that absorbs and retains water within the matrix.[37] Similarly, B3 (169.68%), which contained agar, carrageenan, and corn starch, exhibited relatively high absorption, likely due to the hydrophilic nature of carrageenan. Carrageenan contains sulphate ester groups known to facilitate water binding and swelling in gel networks.[38]

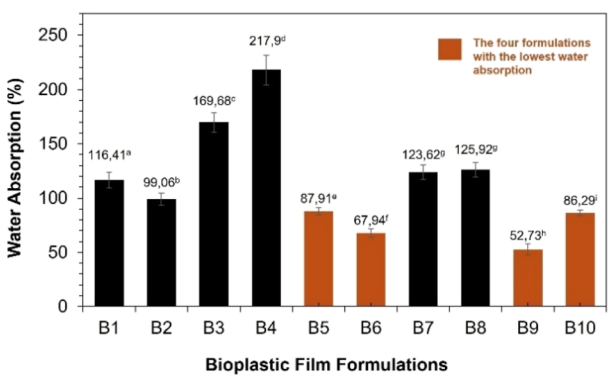

Fig. 1 Water absorption of bioplastic films. Highlighted markers indicate the lowest water absorption values, representing the best water-resistance performance among the tested samples. In the context of straw applications, lower water absorption is considered desirable.

In contrast, the lowest water absorption was found in B9 (52.73%), followed by B6 (67.94%), B10 (86.29%), and B5 (87.91%). In the context of straw applications, lower water absorption values are considered advantageous, as they indicate higher resistance to water penetration and better structural stability during use. These four formulations share key compositional traits: all contain corn starch, while B9 notably excludes carrageenan and konjac, suggesting that the presence of starch alone contributes significantly to reducing hydrophilicity by enhancing network density and reducing porosity.[39] Both B6 and B10 contained carrageenan, while B10 additionally incorporated konjac. These formulations exhibited moderate water absorption, suggesting a complex interplay between the hydrophilic nature of carrageenan and konjac, which may be partially offset by the network-densifying effects of corn starch.

Formulations such as B1 (116.41%), B7 (123.62%), and B8 (125.92%) displayed intermediate water uptake, which could be attributed to their carrageenan content without sufficient balancing by starch or cross-linkers. On the other hand, B2 (99.06%), despite lacking carrageenan, still showed noticeable water uptake likely due to the presence of konjac, reaffirming its strong water-holding characteristics. These findings confirm that careful selection of biopolymer combinations is essential to achieving water-resistant films. Among the tested formulations, B9, which combined agar and corn starch with reinforcing additives (citric acid and $CaCO_3$), offered the most desirable hydrophobic performance. Its superior dimensional stability and low water uptake justify its advancement to the next development phase.

While water absorption was determined in this study, the possible dissolution of low-molecular-weight additives such as sorbitol and citric acid during immersion was not directly quantified. No visible crystallization, whitening, or surface roughening was observed after drying, suggesting minimal migration of these components under the test conditions. Quantification of additive dissolution through chemical analysis of the immersion medium is recommended for future studies to better assess film stability.

Importantly, in this part, four film formulations—B5, B6, B9, and B10—exhibited the lowest water absorption values and were therefore selected for further processing into straw form. The selected candidates will be subjected to comprehensive evaluations in subsequent stages, focusing on thermal, mechanical, and biodegradation performance under optimized mixing conditions.

3.1.2 FTIR characterization of selected bioplastic straw formulations. The functional groups present in the four selected straw formulations (S-B5, S-B6, S-B9, and S-B10) were

identified using Fourier Transform Infrared (FTIR) spectroscopy. These formulations differ in their combinations of agar, carrageenan, corn starch, and calcium carbonate ($CaCO_3$), and were chosen based on their superior water absorption properties. The FTIR spectra, as presented in Fig. 2A, displays key absorption bands corresponding to the biopolymer backbones and the interactions between their components and functional additives.

The FTIR spectra primarily reflected the characteristic functional groups of the constituent polymers and additives, as expected from a formulation prepared by physical blending. Subtle peak shifts and intensity variations were also observed, suggesting possible non-covalent interactions (*e.g.*, hydrogen bonding, electrostatic, or hydrophobic effects) rather than new covalent bonds.

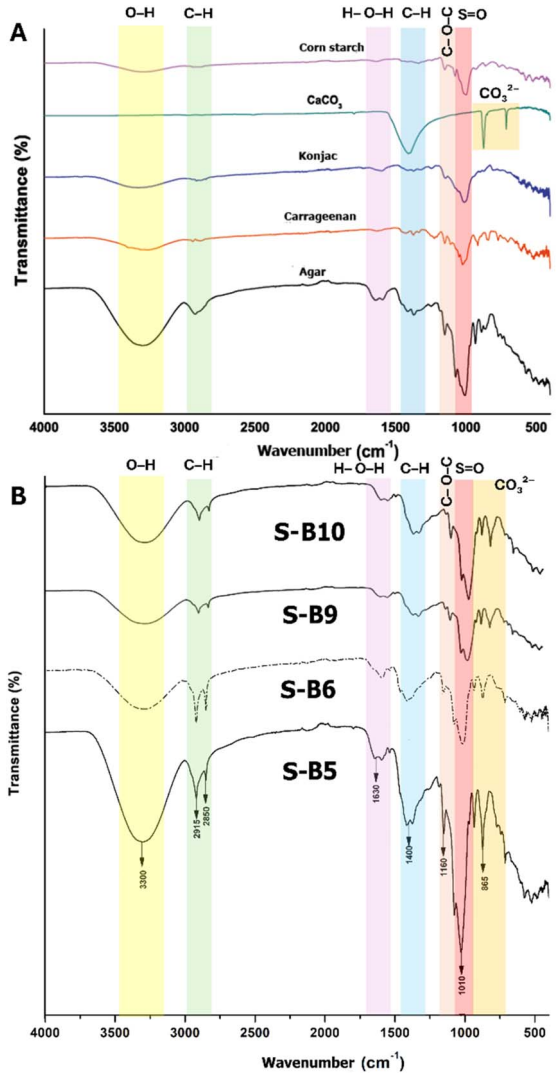

Fig. 2 FTIR spectra of (A) raw components (agar, carrageenan, konjac, corn starch, and $CaCO_3$) and (B) straw formulations (S-B5, S-B6, S-B9, S-B10) with highlighted absorption bands. Yellow: O–H stretching (~3200–3400 cm^{-1}); green: C–H stretching (2850–2920 cm^{-1}); purple: ester C=O (~1730 cm^{-1}); blue: H–O–H bending (~1630 cm^{-1}); red: S=O stretching (1010–1080 cm^{-1}, carrageenan); orange: carbonate peaks (883, 708 cm^{-1}, $CaCO_3$). These bands confirm the presence of each raw material within the straw matrix. The absence of major new peaks suggests that the process is dominated by physical blending rather than extensive chemical reactions.

Fig. 2B reveals that all samples exhibited broad absorption peaks in the range of 3200–3400 cm^{-1}, corresponding to O–H stretching vibrations, which are characteristic of hydroxyl groups in polysaccharides such as agar, carrageenan, and starch. Peaks observed around 2900 cm^{-1} correspond to the C–H stretching vibrations from aliphatic hydrocarbon chains in starch and agar. Notably, formulations B6 and B10, which contain carrageenan, demonstrated absorption bands near 1010–1080 cm^{-1}, confirming the presence of sulphate ester (S=O) functional groups, characteristic of carrageenan, near 1010–1080 cm^{-1}, confirming the presence of sulphate ester (S=O) functional groups, characteristic of carrageenan.[40] These peaks were absent or less pronounced in B5 and B9, which did not include carrageenan, validating the spectral sensitivity to compositional differences.

Formulations S-B5 and S-B6, which include konjac flour, may also contribute unique spectral features. Although konjac's main component, glucomannan, shares similar polysaccharide backbones with agar and starch, it may introduce additional O–H and C–H vibrations due to its highly branched structure. However, its spectral fingerprint typically intersects with other hydrocolloids in the 3200–3400 cm^{-1} and 1000–1200 cm^{-1} regions. Therefore, while its presence may not be distinctly isolated in the FTIR spectra, it may still contribute to the overall hydrogen bonding within the matrix.

Further analysis showed the presence of characteristic bands near 1400–1500 cm^{-1}, as well as distinctive peaks at 883 cm^{-1} and 708 cm^{-1}, particularly in S-B6, S-B9, and S-B10, which confirm the successful incorporation of calcium carbonate ($CaCO_3$) in the form of calcite polymorphs.[41–43] These mineral-based bands were absent in the control films without $CaCO_3$, supporting the structural modification introduced by the additive. In addition, the presence of C–O–C and C–O stretching vibrations was detected in the 1000–1200 cm^{-1} region, typical for polysaccharide backbones. Citric acid's role as a cross-linker may be reflected in slight band shifts and intensity changes in this region, consistent with previous reports at higher concentrations,[44] although in the present formulation the evidence remains indirect.

While FTIR alone cannot conclusively identify these interactions, the observed spectral shifts may suggest contributions from hydrogen bonding among polysaccharides, electrostatic attraction between κ-carrageenan sulphate and Ca^{2+}, and hydrophobic associations involving beeswax. These non-covalent effects are consistent with the improved water resistance and mechanical stability observed in Section 3.3.1. These interactions, while non-covalent, appear to synergistically improve both the mechanical integrity and water resistance of the straws.

Eventually, the FTIR profiles of the four formulations confirm the successful integration of their respective components and validate the formation of physically and chemically compatible biopolymer matrices. These spectral results support the compositional basis for the functional performance

observed in water resistance and mechanical stability, highlighting the selection of S-B5, S-B6, S-B9, and S-B10 for further development into heat-resistant, hydrophobic bioplastic straws.

3.1.3 Surface wettability of selected bioplastic straws. The surface wettability of the four selected straw formulations (S-B5, S-B6, S-B9, and S-B10) was evaluated by measuring their water contact angles, as illustrated in Fig. 3. Among them, S-B9 exhibited the highest contact angle (114.61 ± 1.28°), indicating the most hydrophobic surface, followed by B6 (105.53 ± 2.46°). In contrast, both S-B5 and S-B10 exhibited lower contact angles, likely due to their shared inclusion of konjac flour, which increases the matrix's water affinity. S-B5 and S-B10 showed lower contact angles of 85.09 ± 6.00° and 93.08 ± 1.36°, respectively.

Surface wettability can be categorized based on contact angle values: 0° indicates super-hydrophilic surfaces, 0–90° hydrophilic, 90–120° hydrophobic, 120–150° ultra-hydrophobic, and values greater than 150° correspond to superhydrophobic materials.[45] Based on this classification, S-B9 and S-B6 fall within the hydrophobic category, while S-B5 is closer to the hydrophilic threshold. The posthoc analysis conducted in this part confirmed that the differences in polymer composition, especially carrageenan content, had a significant effect ($p < 0.05$) on contact angle values.

These results align with the earlier FTIR findings, where the presence of sulphate ester (S═O) groups in carrageenan (present in S-B6 and S-B10) contributes to a more hydrophilic surface character. Although both starch and beeswax were included in all four samples and are known to influence surface energy, the differences in wettability are primarily attributed to the presence or absence of carrageenan and konjac. The lower contact angle of S-B5, for instance, is likely related to the hydrophilic behavior of konjac flour, which increases the matrix's water affinity.[46]

It is also important to note that the overall contact angle values (ranging from 85° to 114°) are considerably higher than those reported by Rhim,[24] who observed contact angles of 46–56° for agar–carrageenan blends. This improvement is attributed to the presence of calcium carbonate and beeswax. Calcium carbonate has been shown to improve the hydrophobicity of seaweed-based bioplastics by reducing surface polarity,[33] while beeswax enhances water resistance by lowering hygroscopicity and increasing the water barrier properties.[39] In particular, S-B9, which contains neither carrageenan nor konjac, demonstrated the highest water repellency, supporting its potential as the most suitable formulation for applications requiring minimal water interaction. Similar observations were reported by Cunha and Grenha,[47] who noted that carrageenan increases surface polarity and thus reduces hydrophobicity.

Overall, the enhanced hydrophobic behavior of B9 and B6 suggests their greater suitability for end-use scenarios involving prolonged contact with aqueous media, such as biodegradable drinking straws, where reduced surface wettability is essential to maintain structural integrity and user experience.

3.1.4 Tensile strength and elongation of selected bioplastic straws. The mechanical performance of the four selected straw formulations (S-B5, S-B6, S-B9, and S-B10) was evaluated through tensile strength and elongation testing, as illustrated in Fig. 4. These two parameters are critical indicators of a material's suitability for straw applications, reflecting its ability to withstand deformation and stretching under mechanical stress.

Formulations S-B6 and S-B9 exhibited the highest tensile strength values among the group. S-B6 achieved 93.35 MPa, while S-B9 followed with 73.33 ± 6.01 MPa. These values are substantially higher than those reported in previous agar-based bioplastic studies,[21,48,49] indicating the structural reinforcing effect of calcium carbonate, starch, and beeswax. S-B6's superior strength can also be attributed to the controlled ratio of agar and carrageenan, with corn starch acting as a densifying filler that enhances network compactness.

In contrast, S-B5 and S-B10 displayed lower tensile strength values—44.40 MPa and 45.04 ± 1.92 MPa, respectively—suggesting that the presence of konjac or higher carrageenan content may compromise the polymer matrix uniformity. Konjac's water-binding nature can lead to microstructural inconsistencies, while excessive carrageenan disrupts agar's cohesive gel network.[21,50] Elongation at break was significantly higher in formulations S-B5 (~61%) and S-B10 (~62.00), indicating

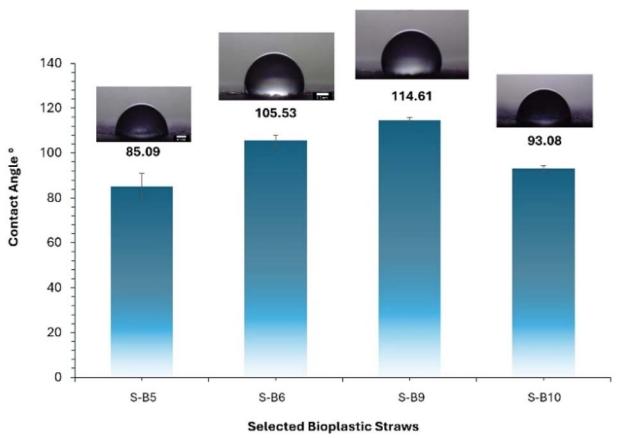

Fig. 3 Surface wettability of selected bioplastic straws.

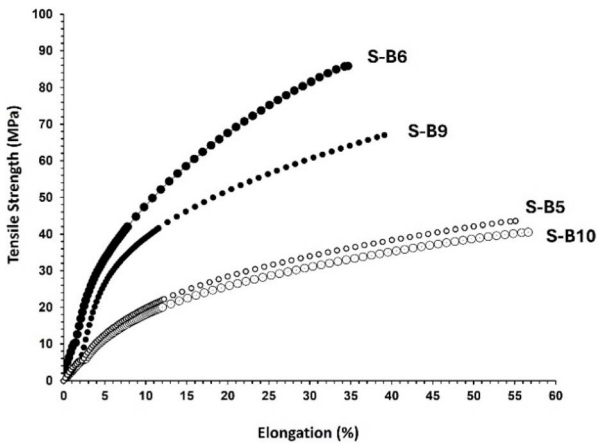

Fig. 4 Tensile strength and elongation of selected bioplastic straws.

enhanced flexibility attributed to the plasticizing effect of sorbitol and the structural contributions of konjac and carrageenan. In contrast, S-B6 (~39%) and S-B9 (~40) exhibited markedly lower elongation, suggesting increased stiffness and reduced extensibility in these biopolymer matrices.

These results illustrate a trade-off between tensile strength and elongation: S-B6 and S-B9 offered strong and rigid structures, ideal for maintaining straw integrity under stress, while S-B5 and S-B10 provided more elastic, flexible profiles. This balance between strength and flexibility is critical in tailoring bioplastic straw properties for consumer usability and durability during application. Overall, the findings validate the formulation strategies used in the development of S-B6 and S-B9 as strong candidates for durable bioplastic straws, while S-B5 and S-B10 may be optimized for scenarios where enhanced elasticity is desired.

3.1.5 Thermal degradation behavior of bioplastic straw formulations. The thermal degradation behavior of four bioplastic straw formulations (S-B5, S-B6, S-B9, and S-B10) was evaluated using thermogravimetric analysis (TGA), derivative thermogravimetry (DTG), and differential thermal analysis (DTA), as shown in Fig. 5. All formulations exhibited multi-step degradation patterns, which are characteristic of polysaccharide-based bioplastics.[33,51,52] Each degradation event provides critical insight into the compositional effect of agar, starch, carrageenan, konjac, and additives on thermal performance.

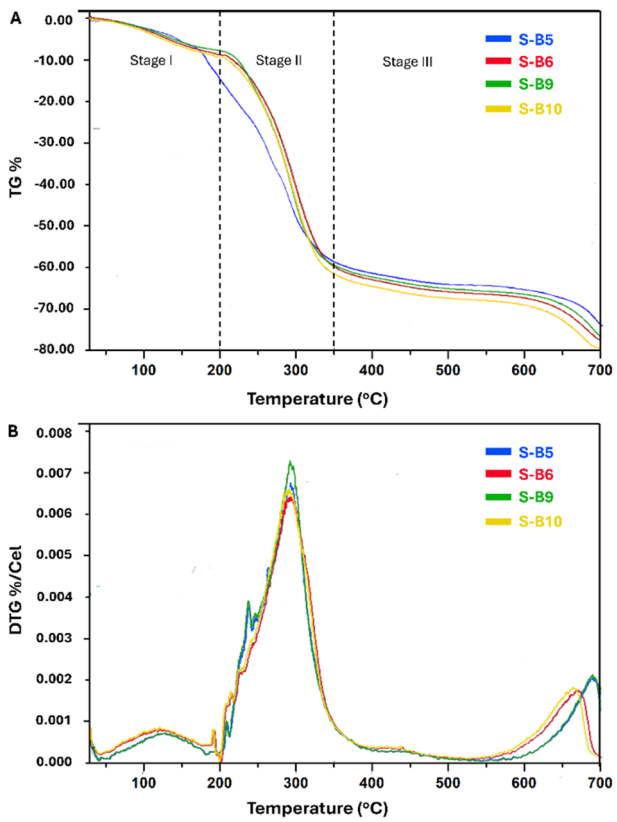

Fig. 5 Thermogravimetric analysis (TGA) and derivative thermogravimetry (DTG) curves of straw formulations (S-B5, S-B6, S-B9, and S-B10). (A) TGA curves showing the percentage weight loss as a function of temperature. (B) DTG curves indicating the degradation rate and maximum decomposition temperatures (T_{max}) of each formulation. These results confirm multi-step degradation behavior, corresponding to initial moisture loss, polymer backbone decomposition, and final residue stabilization.

Stage I (below ~200 °C) reflected initial weight loss due to moisture evaporation. The S-B5 sample exhibited the highest weight reduction in this phase, likely due to its higher konjac content, a hydrocolloid known for its pronounced hygroscopicity. S-B10, which also contains konjac, showed moderate moisture loss, higher than S-B6 and S-B9 but lower than S-B5. This suggests partial hygroscopic behavior influenced by konjac concentration and matrix interaction.

Stage II (200–350 °C) was the primary degradation phase, during which polysaccharide chains underwent depolymerization and volatile components—including sorbitol, beeswax, and citric acid—were released. Among all samples, S-B9 exhibited the latest degradation onset and a relatively gradual decomposition profile, indicating greater matrix stability. This behavior is likely due to the combination of agar and starch without thermally labile hydrocolloids such as carrageenan or konjac. Moreover, the presence of calcium carbonate is thought to contribute to thermal shielding and char-promoting effects, enhancing the structural rigidity and stabilizing the degradation pathway.[53]

In contrast, S-B6 and S-B10, both containing carrageenan, showed slightly earlier thermal degradation onset and sharper mass loss slopes. This result is in line with the literature, where carrageenan's sulphated ester groups are thermally unstable and begin to decompose at lower temperatures than agar. S-B5, which includes konjac but no carrageenan, exhibited the most rapid and intense decomposition in this stage, reinforcing the thermolabile nature of glucomannan-based materials.

Stage III (>400 °C) corresponds to the breakdown of remaining carbonaceous structures and the formation of thermally stable residues. Here, S-B9 left the highest final residue (~27%), followed by B10 (~25.5%), S-B6 (~24%), and S-B5 (~22%). These residual trends are in agreement with microstructure (Fig. 6) and reflect the importance of both initial matrix composition and additive interactions in preserving structural coherence upon exposure to high temperatures. The incorporation of inorganic fillers like $CaCO_3$ further contributed to residue formation by acting as a non-volatile matrix stabilizer and promoting carbonaceous char formation.

The DTG profiles revealed a clear differentiation in decomposition peaks. S-B9 displayed a sharp single degradation peak between 290–310 °C, while S-B6 and S-B10 showed broader or shoulder peaks, consistent with the overlapping thermal breakdown of carrageenan and other polymers. S-B5 and S-B10 both exhibited broadened DTG peaks with early shoulders around 260–280 °C, indicative of konjac's early decomposition. The overlap with carrageenan breakdown in S-B10 resulted in a slightly smeared double-peak profile, reflecting complex thermal interactions between these thermolabile polysaccharides.

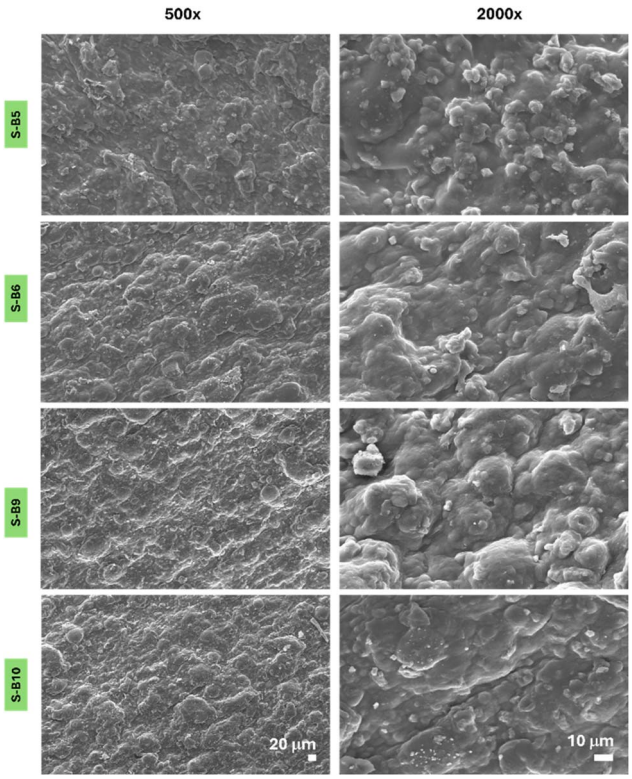

Fig. 6 SEM micrographs of selected bioplastic straw formulations (S-B5, S-B6, S-B9, and S-B10) at 500× and 2000× magnification.

Furthermore, DTA curves demonstrated the exothermic and endothermic nature of each decomposition phase. S-B9 exhibited the most defined endothermic peak at higher temperature ranges, suggesting more stable energy absorption prior to thermal collapse. B5 showed weaker and earlier DTA transitions, once again underlining its lower thermal integrity.

3.1.6 Microstructure analysis of selected bioplastic straws. The microstructure of selected straw formulations (S-B5, S-B6, S-B9, and S-B10) was investigated using Scanning Electron Microscopy (SEM) at a magnification of 2000× to observe the morphological features at the microscale. The SEM analysis focused on assessing film continuity, interfacial adhesion, component dispersion, and evidence of phase separation within the biopolymer matrix. These micrographs are presented in Fig. 6.

Among the samples, S-B9—formulated with 7.5 g agar and no carrageenan or konjac—exhibited the most cohesive and moderately compact matrix morphology. While some granular texture and surface unevenness were observed, the overall structure appeared more continuous and less porous compared to the other samples. This relatively uniform microstructure suggests favorable interpolymer compatibility and filler dispersion.

In contrast, S-B5, which incorporates 1.5 g konjac, presented a more porous and fibrous morphology. The surface was interspersed with irregular voids and microchannels, which can be attributed to konjac's strong hydrophilicity and swelling behavior during drying. Konjac's inclusion likely disrupted the uniform matrix formation, as its tendency to bind water and form gels can lead to localized phase expansion followed by collapse upon dehydration. This porous morphology may have facilitated greater water penetration, as supported by higher water absorption and elongation values in the physical tests. However, this structure could be beneficial in applications demanding flexibility or permeability.

S-B6, which replaces konjac with 2.5 g carrageenan, displayed more fractured and heterogeneous regions, including distinct microcracks and particle aggregation zones. These surface defects point to poor compatibility between carrageenan and starch in the presence of agar, possibly due to differences in charge distribution and polymeric chain interaction. The observed cracks and discontinuities indicate weak interfacial adhesion and inefficient plasticizer distribution, which may explain S-B6's relatively low elongation at break and moderate tensile strength.

Interestingly, S-B10 showed a heterogeneous yet slightly smoother surface compared to S-B6. Despite some irregularities, the combination of konjac and carrageenan may have improved interpolymer blending to a modest extent. However, notable surface granularity and unevenness remain, indicating that matrix integration was only partially achieved. These morphological features align with the intermediate mechanical and water barrier properties observed in S-B10.

Across all samples, residual calcium carbonate particles were occasionally visible, appearing as bright, unevenly distributed granules. These may have originated from partial sedimentation during casting or incomplete interaction with the polymer matrix. However, no visible trapped air bubbles or significant delamination were observed, indicating that the homogenization and degassing procedures during straw formation were effective. The beeswax, although not visually distinguishable in SEM, likely contributed to surface hydrophobicity and acted as a compatibilizer, improving the overall matrix integrity. Taken together, these microstructural observations corroborate the physicochemical trends previously discussed which were S-B9's structural compactness, S-B5's fibrous porosity, S-B6's phase separation, and B10's intermediate integration, demonstrating that component selection and blending strategy play a decisive role in determining the morphological and functional performance of biodegradable straw materials.

3.2 Homogenization optimization and straw performance

Based on a comprehensive evaluation of surface wettability (contact angle), tensile elongation, thermal degradation behavior, and microstructural integrity, formulation S-B9 was selected as the most promising candidate for further process optimization. S-B9 exhibited the highest contact angle, indicating improved surface hydrophobicity; superior tensile strength with acceptable elongation; a delayed onset of thermal degradation; and a compact, homogeneous matrix with minimal phase separation under SEM analysis. These combined properties demonstrate enhanced polymer–filler compatibility and structural stability, making S-B9 the most suitable formulation to proceed into the homogenization

optimization stage for process refinement and performance enhancement.

To further enhance its functional properties and production consistency, S-B9 was subjected to homogenization treatment using an overhead stirrer (characterized by lower speeds, <10 000 rpm) under varying speed and time conditions. A two-level factorial experimental design was employed, incorporating three independent variables: temperature (60–80 °C), stirring speed (1500–2000 rpm), and mixing time (15–45 minutes). Eleven treatment combinations were executed, as presented in Tables 3 and 4. The low-speed homogenization variant was referred to as low-speed S-B9, and the results of these optimization trials are presented in the following subsections.

3.2.1 Water absorption performance of straw samples. Water absorption is a key parameter for quantifying the water resistance of biodegradable straws and predicting their dimensional stability during use. In this study, the percentage of weight gain was measured after immersion in normal water (90 minutes) and hot water (85 °C for 30 minutes). Lower absorption indicates better barrier performance, reduced swelling, and improved product stability. The results from experimental runs are presented in Fig. 7.

Previously, the S-B9 formulation, while effective in producing hydrophobic and thermally resistant straws at the lab scale, relied on high-shear homogenization (>10 000 rpm). This posed practical limitations for industrial scaling due to high energy consumption, limited batch capacity, and operational safety concerns. To overcome this, a low-speed overhead homogenization strategy was implemented, aiming to preserve or improve product functionality while enhancing process feasibility.

A 3^2 factorial design was applied to evaluate the effects of homogenization speed (1500, 1750, and 2000 rpm), homogenization temperature (60–80 °C), and time (15, 30, 45 minutes) on straw performance. The matrix formulation was based on B9, previously identified as the most robust due to its compact microstructure, high contact angle, and thermal resilience. The optimization strategy aimed to maintain these characteristics under modified processing conditions. As shown in Fig. 7, water absorption values varied across treatment combinations. LLH recorded the lowest absorption in normal water (94.03 ± 0.64%), while LHL showed the highest (110.15 ± 6.08%). In hot water, HLL achieved the lowest absorption (100.27 ± 2.67%), while HHL reached 137.71 ± 2.23%.

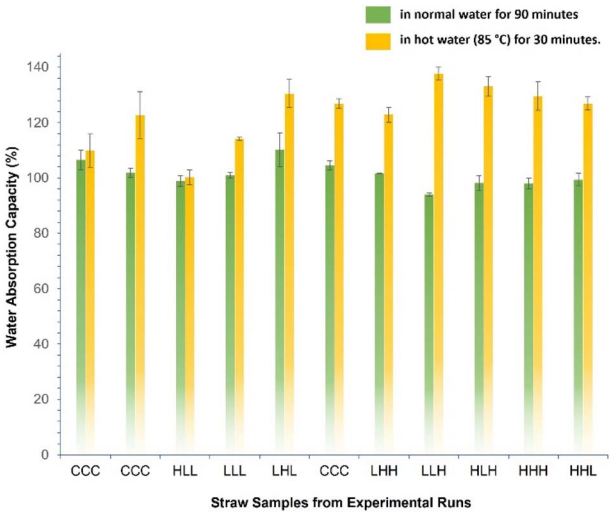

Fig. 7 Water absorption of S-B9-based straws after low-speed homogenization (using overhead stirrer). Samples were immersed in normal water (90 min) and hot water at 85 °C (30 min), with straws produced under varying homogenization temperature (60–80 °C), stirring speed (1500–2000 rpm), and mixing time (15–45 minutes).

Comparative analysis with high-speed homogenization revealed a notable improvement: the high-shear control sample absorbed up to 135.51 ± 2.83%, significantly higher than the best-performing low-speed straw (HLL). This suggests that gentle mixing supports more uniform $CaCO_3$ and beeswax distribution, forming a denser matrix with fewer internal voids that typically promote water ingress. This effect aligns with prior findings that $CaCO_3$ and lipid-based additives enhance water resistance by increasing matrix packing and reducing capillary diffusion paths.[54] The HLL straw exhibited similar water absorption capacities in both normal water immersion (98.96 ± 1.93%) and hot water immersion (100.27 ± 2.67%). This finding supports its functionality for use in both cold and hot beverages and aligns with ISO 18188:2016 standards regarding straw resistance to extreme temperatures (both hot

Table 4 Comparison of physical and mechanical properties of selected low-speed-S-B9 straw, high-speed-S-B9 straw, and commercial paper straw[a]

Parameters	Selected low-speed-S-B9 straw	High-speed-S-B9 straw	Commercial paper straw
Thickness (mm)	0.67 ± 0.01[a]	0.68 ± 0.01[a]	0.56 ± 0.02[b]
Water absorption (%)	100.27 ± 2.67[a]	115.51 ± 2.83[b]	120.1 ± 1.91[c]
Water solubility (%)	5.20 ± 1.25[a]	4.87 ± 0.40[a]	8.35 ± 1.44[b]
Contact angle (°)	115.31 ± 1.15[a]	113.36 ± 3.98 [ab]	103.12 ± 1.64[c]
Tensile strength (MPa)	60.76 ± 2.78[a]	73.33 ± 2.17[b]	56.10 ± 2.63[c]
Elongation (%)	34.61 ± 2.45[a]	33.53 ± 2.85[a]	11.95 ± 0.53[b]
Flexural strength (MPa)	4.72 ± 2.09[a]	4.61 ± 1.07[a]	5.72 ± 0.18[b]

[a] Note: values are expressed as mean ± standard deviation ($n = 3$). Different superscript letters (a–c) within the same row indicate significant differences at $p < 0.05$ (Tukey's HSD test).

and cold). Altogether, the results confirm that low-speed overhead homogenization not only offers an energy-efficient, scalable alternative to high-shear processes, but can produce straws with comparable or superior water resistance. The HLL treatment, combining 80 °C, 15 minutes, and 1500 rpm, was identified as the most effective condition for future industrial application.

3.3 Comparative analysis of selected bioplastic straw characteristics

The selected HLL formulation (now coded as a selected low-speed-S-B9 straw) was then compared with the previous B9-based straw (high-speed S-B9 straw) and a commercial paper straw, in order to benchmark its structural integrity and functional performance against both research-grade and market-standard references. The comparison was conducted to evaluate whether the developed bioplastic straw possesses characteristics and performance comparable to commercial products and those produced using high-speed homogenization. Observed parameters included visual appearance and thickness, as well as functional attributes such as water absorption, tensile strength, elongation, flexibility (bending), contact angle, and straw degradability, as shown in the comparative data in Table 4.

Compared with the commercial paper straw, the optimized low-speed-S-B9 straw showed ~16.5% lower water absorption, a 12.3° higher contact angle, and nearly three times greater elongation, indicating improved water resistance and flexibility. Polylactic acid (PLA) straws, another widely promoted biodegradable alternative, can reach similar tensile strength but require high-temperature extrusion and degrade more slowly (>180 days) than the 60 days observed here. While the predicted production cost of the seaweed-based straw at a scaled-up level is still higher than PLA at present, the use of moderate processing temperatures (≤95 °C) and locally sourced seaweed offers potential for future cost reductions through process optimization and economies of scale.

3.3.1 Visual characteristics. Appearance is one of the most critical sensory attributes influencing consumer perception of a product. It encompasses characteristics such as color, size, shape, and surface texture,[55] and the intrinsic properties of constituent materials strongly influence the final product's appearance. The selected low-speed S-B9 straw exhibited a light brownish-white color, a surface speckled with fine white dots, a firm structure, and moderate flexibility when bent. In comparison, the high-speed S-B9 straw displayed a dull white color with a smooth and homogeneous surface texture, robust form, and the ability to bend up to 90°. Meanwhile, commercial paper straws presented a visually appealing multicolored surface with visible spiral seams along the length but showed limited elasticity. The comparative visual appearances of the selected low-speed S-B9 straw, paper straw, and high-speed S-B9 straw are presented in Fig. 8.

The surface speckling observed on the selected low-speed S-B9 straw is attributed to suboptimal homogenization during the mixing process. The overhead stirrer employed in this study

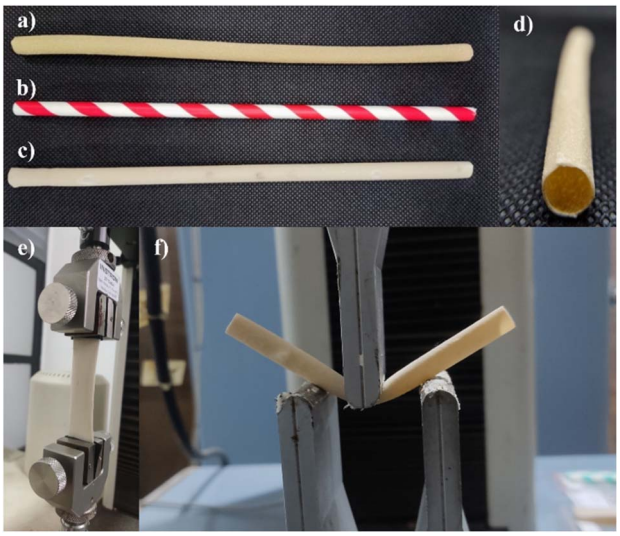

Fig. 8 Visual and mechanical evaluation of straw samples: (a) selected low-speed S-B9 straws, (b) commercial paper straws, (c) high-speed S-B9 straws, (d) mouth-end cross-sectional appearance, (e) tensile testing setup, and (f) three-point bending test setup of the selected straw.

operates at low rotational speeds (1500–2000 rpm) and relies on high torque for material blending. It uses a direct current (DC) motor to drive the submerged rotor, enabling controlled shear mixing. This contrasts with the high-shear disperser homogenizer used by high-speed-S-B9 straw, which operates at speeds ranging from 10 000 to 20 000 rpm. These devices apply intense shear forces through a rotor–stator mechanism powered by motors up to 100 horsepower (hp), forcing fluid flow directly through the impeller axis.

Straws produced using the high-shear homogenizer demonstrated more uniform morphology compared to those processed with an overhead stirrer. The rotor–stator system subjects the medium to axial entry and radial discharge through a narrow gap between the rotor and stator, generating intense friction and particle size reduction. This process results in efficient dispersion and microstructural homogeneity. In contrast, overhead stirring promotes circular flow patterns, where the mixture cycles from the impeller down to the base and back upward, resulting in less intense mixing, while homogenizer flow is concentrated directly toward the rotor–stator axis.

3.3.2 Thickness, water absorption, and contact angle comparison. The surface wettability measurements discussed in this section were performed on the optimized straw formulation derived from the low-speed homogenization process (selected low-speed-S-B9), the high-shear homogenized straw (high-speed-S-B9) and a commercial paper straw for comparative analysis. According to Table 4, the thickness values of the selected low-speed-S-B9 (0.67 mm) and high-speed-S-B9 (0.68 mm) did not differ significantly, suggesting comparable dimensional properties regardless of homogenization method. In contrast, the commercial paper straw had a significantly lower thickness (0.56 ± 0.02 mm). Water absorption results also

revealed statistically significant differences: the selected low-speed-S-B9 straw absorbed significantly less water (100.27%) than both the high-speed-B9 straw (115.51%) and the commercial paper straw (120.1%). These findings validate the superior barrier performance of the low-speed straw, likely attributed to more efficient integration and orientation of hydrophobic additives (*e.g.*, beeswax and $CaCO_3$) under gentle mixing conditions, which reduce porosity and limit capillary water penetration.

The contact angle data provides further insight into surface hydrophobicity across the straw samples. Both the selected low-speed-S-B9 and high-speed-S-B9 straws exhibited similarly high contact angle values (113–115°), indicating no significant difference in their surface water repellency. In contrast, the commercial paper straw demonstrated a slightly lower contact angle (103°), placing it well below the hydrophobic performance of the bioplastic-based alternatives. The consistently higher hydrophobicity of both bioplastic straws, relative to the commercial control, reinforces their potential for superior resistance to wetting and prolonged structural integrity in moist environments. This increase was likely due to more stable surface structuring, calcium carbonate and wax distribution, as high-speed shear may disrupt the polar–nonpolar interface, reducing surface repellence. Following Bracco and Holst,[56] surfaces with contact angles between 90° and 120° are considered hydrophobic, while those above 120° are classified as ultra-hydrophobic. Importantly, the lower-speed process achieved a level of quality comparable to, or even exceeding, that of the high-speed and commercial products, particularly within the hydrophobicity range typical of coated paper straws. Additionally, visual inspection in Fig. 9 showed that after 4 hours of soaking, both the selected low-speed-S-B9 and high-speed-S-B9 straws maintained their shape and structural integrity equally well, in contrast to the commercial straw, which exhibited noticeable deformation. This visual evidence supports the quantitative data and highlights the superior moisture resistance of the bioplastic formulations compared to the paper-based control.

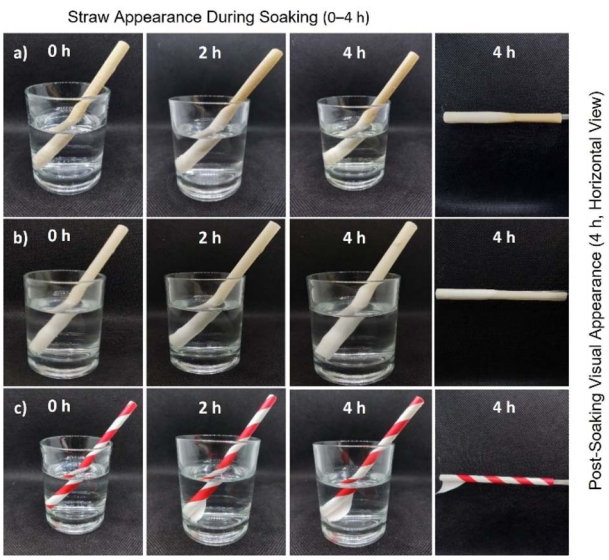

Fig. 9 Visual comparison of straw appearance during immersion in water over time and after 4 hours (side view). (a) Selected low-speed S-B9 straws, (b) high-speed S-B9 straws, (c) commercial plastic-coated paper straw. Left panels show time-lapse images at 0, 2, and 4 hours of soaking in water. Right panels display the horizontal (side) view of each straw after 4 hours. The 4 h immersion represents an accelerated stress test far exceeding typical usage duration (30–60 min) and is intended to compare relative water-resistance performance under extreme conditions.

3.3.3 Water solubility. The selected Low-speed-S-B9 exhibited low water solubility values (5.20 ± 1.25%), which were comparable to those of the high-speed-S-B9 (4.87 ± 0.40%) ($p > 0.05$) and significantly lower than those of the commercial paper straw (8.35 ± 1.44%) ($p < 0.05$). Together with the high contact angle (>110°) and the preserved structural integrity after soaking, these findings suggest that the straw matrix primarily undergoes water uptake through swelling rather than dissolution, thereby minimizing the release of soluble fractions into beverages and confirming limited leaching of solids. A previous report demonstrated higher water solubility (~100%), in which a polysaccharide-based polymer complex composed of chitosan, sodium alginate, and carboxymethyl cellulose (CMC) fully dissolved after 24 h.[57] In addition, the present study shows a lower solubility compared to that of polylactic acid (PLA)-based biofilms, as reported by Krishnamurthy and Amritkumar.[36]

3.3.4 Mechanical and flexural properties. The mechanical and flexural performance of the straw samples was evaluated to compare the effects of different homogenization speeds. As shown in Table 4, the High-Speed-S-B9 straw exhibited the highest tensile strength (73.33 MPa), followed by the selected low-speed-S-B9 (60.76 MPa) and the commercial paper straw (56.10 MPa). Although high-speed processing provided an advantage in tensile load-bearing, both B9-based straws remained mechanically superior to the commercial counterpart (Fig. 8e).

In terms of elongation, the selected low-speed-S-B9 and high-speed-S-B9 straws performed similarly, with values of 34.61% and 33.53%, respectively. Both formulations exhibited substantially greater ductility than the commercial straw (11.95%), indicating better flexibility and energy absorption under stress—key attributes of straw for everyday usability. Flexural strength showed no substantial difference among the samples. The commercial paper straw recorded a value of 5.72 MPa, which was comparable to the selected low-speed-S-B9 (4.72 MPa) and high-speed-S-B9 (4.61 MPa). Despite slight numerical variation, all three straws demonstrated similar bending resistance (Fig. 8f).

3.3.5 Biodegradability assessment. To determine the environmental compatibility of the developed straws, a biodegradability test was conducted over a 60-day soil burial period as shown in Fig. 10. The assessment focused on the optimized low-speed homogenized straw and the standard high-shear homogenized straw, both formulated with the agar based. Additionally, commercial paper straws were included as a control.

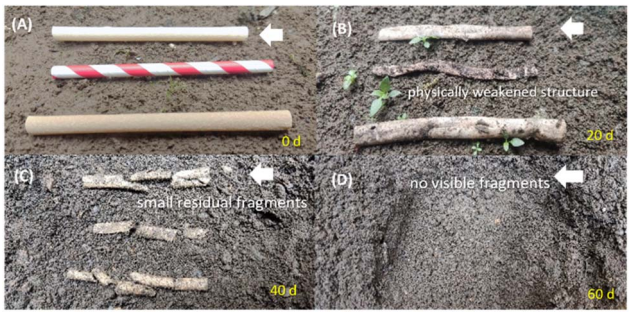

Fig. 10 Degradability testing of selected low-speed S-B9 straws, commercial plastic-coated paper straw, and high-speed S-B9 straws (from bottom to top): (A) 0 days after burial in soil; (B) 20 days after burial; (C) 40 days after burial; (D) 60 days after burial.

Visual inspection and structural analysis revealed distinct degradation patterns. On day 0, all straws retained full structural integrity. By day 20, the low-speed and high-shear straws began to exhibit signs of surface erosion and small cavities, while the paper straw displayed discoloration and early signs of delamination. By day 40, the bioplastic straws showed significant breakdown with large areas of fragmentation, and the paper straw had become highly brittle. On day 60, both bioplastic straw types were fully degraded and no longer identifiable in the soil, whereas remnants of the paper straw were still observable. These findings align with prior reports indicating that starch-based bioplastics are highly susceptible to microbial degradation in moist and aerated environments.[58] The presence of polysaccharides such as agar and starch, coupled with biodegradable plasticizers and fillers, enhances microbial enzymatic activity, promoting complete material breakdown. Notably, the similar degradation profiles between low-speed and high-shear straws further affirm that the process optimization did not impair the material's composability. The observed biodegradation performance confirms the environmental viability of the developed seaweed derived straws and supports their application as a sustainable alternative to synthetic polymer-based single-use straws.

4 Conclusions

This study developed a biodegradable bioplastic straw using seaweed-based biopolymers, with particular emphasis on agar–starch formulations reinforced with calcium carbonate and beeswax. Among the tested compositions, the B9 formulation (comprising 7.5 g agar and 5.35 g corn starch, without carrageenan or konjac) showed structural homogeneity, higher thermal resistance, and higher hydrophobicity compared with the other formulations. Optimization *via* factorial design demonstrated that low-speed homogenization at 80 °C for 15 minutes at 1500 rpm enhanced matrix integration and improved surface characteristics while maintaining mechanical strength. The optimized B9 straw achieved a contact angle of 114°, water uptake of approximately 100%, tensile strength of around 60 MPa, and flexural performance comparable to commercial paper straws. Soil burial testing confirmed complete disintegration within 60 days. These results indicate that the optimized B9 formulation has potential as a scalable and sustainable alternative to petroleum-based single-use drinking straws.

Author contributions

Wahyu Ramadhan: conceptualization (supporting); writing – original draft (lead). Uju – editing & reviewing (supporting); conceptualization (lead); funding acquisition (lead); project administration (lead). Joko Santoso: reviewing draft (supporting); conceptualization (lead); funding acquisition (lead); project administration (lead), investigation (supporting); supervision (equal). Rahadiyan Garuda Langit Dewangga: funding acquisition (lead); project administration (lead). Mario Natanael: data curation (lead); writing – original draft (supporting). Muhammad Aldy Luthfiansyah: data curation (supporting); writing – original draft (supporting). Adinda Yulya Rachmawati: data curation (supporting); project administration (supporting). Zacky Arivaie Santosa: data curation (supporting); project administration (supporting).

Conflicts of interest

No potential conflict of interest was reported by the author(s).

Data availability

All data supporting the findings of this study are available from the corresponding author on reasonable request.

Acknowledgements

The authors gratefully acknowledge the support from the Kedaireka Matching Fund 2023 under Grant No. 13267/IT3.L1/HK.07.00/P/T/2023 and 21/E1/HK.02.02/2023, provided by the Directorate General of Higher Education, Research, and Technology (DIKTI), Ministry of Education, Culture, Research, and Technology, Republic of Indonesia. This research was conducted in collaboration with PT Ijo Inovasi Indonesia to support the development of commercially viable and sustainable seaweed-based bioplastic straws for the Indonesian market.

References

1 P. G. C. Nayanathara Thathsarani Pilapitiya and A. S. Ratnayake, The world of plastic waste: A review, *Cleaner Mater.*, 2024, **11**, 100220.
2 J. R. Jambeck, R. Geyer, C. Wilcox, T. R. Siegler, M. Perryman, A. Andrady, R. Narayan and K. L. Law, Plastic waste inputs from land into the ocean, *Science*, 2015, **347**, 768–771.
3 R. Geyer, J. R. Jambeck and K. L. Law, Production, use, and fate of all plastics ever made, *Sci. Adv.*, 2017, **3**(7), e1700782.
4 J. P. da Costa, The 2019 global pandemic and plastic pollution prevention measures: Playing catch-up, *Sci. Total Environ.*, 2021, **774**, 145806.

5 K. Rana, A Comparative Life-Cycle, Socio-Economic, and Policy Analysis of Alternatives to Plastic Straws, Master's thesis, Michigan Technological University, 2020.
6 S. Gibbens, A brief history of how plastic straws took over the world, *National Geographic*, 2019, available at: https://www.nationalgeographic.com/environment/article/news-plastic-drinking-straw-history-ban, accessed May 2, 2025.
7 X. Zhao, Y. Wang, X. Chen, X. Yu, W. Li, S. Zhang, X. Meng, Z.-M. Zhao, T. Dong, A. Anderson, A. Aiyedun, Y. Li, E. Webb, Z. Wu, V. Kunc, A. Ragauskas, S. Ozcan and H. Zhu, Sustainable bioplastics derived from renewable natural resources for food packaging, *Matter*, 2023, **6**, 97–127.
8 S. Hussain, R. Akhter and S. S. Maktedar, Advancements in sustainable food packaging: from eco-friendly materials to innovative technologies, *Sustainable Food Technol.*, 2024, **2**, 1297–1364.
9 C. G. Otoni, H. M. C. Azeredo, B. D. Mattos, M. Beaumont, D. S. Correa and O. J. Rojas, The Food–Materials Nexus: Next Generation Bioplastics and Advanced Materials from Agri-Food Residues, *Adv. Mater.*, 2021, **33**(43), 2102520.
10 T. D. Moshood, G. Nawanir, F. Mahmud, F. Mohamad, M. H. Ahmad and A. AbdulGhani, Sustainability of biodegradable plastics: New problem or solution to solve the global plastic pollution?, *Curr. Res. Green Sustainable Chem.*, 2022, **5**, 100273.
11 T. Rasheed, S. H. Vattathurvalappil, M. M. Shaukat, R. Theravalappil, U. Ali, A. C. Ummer, M. T. Bin Saleem, E. A. Jaseer and M. Imran, Recent updates on biodegradability and recyclability of bioplastics - Towards a new era in sustainability, *Sustainable Mater. Technol.*, 2024, **41**, e01051.
12 M. Malhotra, N. Garg, P. Chand and A. Jakhete, in *Valorization of Biomass to Bioproducts*, Elsevier, 2023, pp. 475–504.
13 B. B. Sedayu, M. J. Cran and S. W. Bigger, A Review of Property Enhancement Techniques for Carrageenan-based Films and Coatings, *Carbohydr. Polym.*, 2019, **216**, 287–302.
14 A. Panou and I. Karabagias, Biodegradable Packaging Materials for Foods Preservation: Sources, Advantages, Limitations, and Future Perspectives, *Coatings*, 2023, **13**, 1176.
15 J. R. A. Pires, V. G. L. Souza, P. Fuciños, L. Pastrana and A. L. Fernando, Methodologies to Assess the Biodegradability of Bio-Based Polymers—Current Knowledge and Existing Gaps, *Polymers*, 2022, **14**, 1359.
16 M. P. Sudhakar, V. D. Nallasamy, G. Dharani and A. H. Buschmann, Applications of seaweed biopolymers and its composites in dental applications, *J. Appl. Biol. Biotechnol.*, 2024, **12**(1), 62–68.
17 P. Tennakoon, P. Chandika, M. Yi and W.-K. Jung, Marine-derived biopolymers as potential bioplastics, an eco-friendly alternative, *iScience*, 2023, **26**, 106404.
18 M. A. Budiman, Uju and K. Tarman, A Review on the difference of physical and mechanical properties of bioplastic from seaweed hydrocolloids with various plasticizers, *IOP Conf. Ser. Earth Environ. Sci.*, 2022, **967**, 012012.
19 A. Nesic, S. Meseldzija, S. Benavides, F. A. Figueroa and G. Cabrera-Barjas, Seaweed as a Valuable and Sustainable Resource for Food Packaging Materials, *Foods*, 2024, **13**, 3212.
20 Uju, J. Santoso, W. Ramadhan and M. F. Abrory, Extraction of native agar from *Gracillaria* sp with ultrasonic acceleration at low temperature, *J. Pengolah. Has. Perikan. Indones.*, 2018, **21**, 414–422.
21 V. Hernández, D. Ibarra, J. F. Triana, B. Martínez-Soto, M. Faúndez, D. A. Vasco, L. Gordillo, F. Herrera, C. García-Herrera and A. Garmulewicz, Agar Biopolymer Films for Biodegradable Packaging: A Reference Dataset for Exploring the Limits of Mechanical Performance, *Materials*, 2022, **15**, 3954.
22 A. M. M. Sousa and M. P. Gonçalves, Strategies to improve the mechanical strength and water resistance of agar films for food packaging applications, *Carbohydr. Polym.*, 2015, **132**, 196–204.
23 S. Shankar, J. P. Reddy and J.-W. Rhim, Effect of lignin on water vapor barrier, mechanical, and structural properties of agar/lignin composite films, *Int. J. Biol. Macromol.*, 2015, **81**, 267–273.
24 J.-W. Rhim, Physical-Mechanical Properties of Agar/κ-Carrageenan Blend Film and Derived Clay Nanocomposite Film, *J. Food Sci.*, 2012, **77**(12), N66–N73.
25 R. Meena, K. Prasad and A. K. Siddhanta, Development of a stable hydrogel network based on agar–kappa-carrageenan blend cross-linked with genipin, *Food Hydrocolloids*, 2009, **23**, 497–509.
26 Z. Wu, Y. Kong, T. He, Y. Li, Z. Kang, F. Xie and T. Liu, Mechanism of interaction between agar and corn starch: Towards improved properties of starch-based cryogel, *Food Hydrocolloids*, 2024, **150**, 109672.
27 Y. Guo, B. Zhang, S. Zhao, D. Qiao and F. Xie, Plasticized Starch/Agar Composite Films: Processing, Morphology, Structure, Mechanical Properties and Surface Hydrophilicity, *Coatings*, 2021, **11**, 311.
28 R. Zhang, W. Wang, H. Zhang, Y. Dai, H. Dong, L. Kong and H. Hou, Effects of preparation conditions on the properties of agar/maltodextrin-beeswax pseudo-bilayer films, *Carbohydr. Polym.*, 2020, **236**, 116029.
29 L. F. B. Nogueira, B. C. Maniglia, L. S. Pereira, D. R. Tapia-Blácido and A. P. Ramos, Formation of carrageenan-CaCO 3 bioactive membranes, *Mater. Sci. Eng. C*, 2016, **58**, 1–6.
30 L. Nuriyah, G. Saroja and J. Rohmad, The Effect of Calcium Carbonate Addition to Mechanical Properties of Bioplastic Made from Cassava Starch with Glycerol as Plasticizer, *IOP Conf. Ser.:Mater. Sci. Eng.*, 2019, **546**, 042030.
31 M. Kozlowski, The Formation of Interpenetrating Polymer Blends, *J. Polym. Eng.*, 1995, **14**(1), 15–41.
32 P. Salum, Ç. Ulubaş, O. Güven, M. Cam, L. Y. Aydemir and Z. Erbay, The Impact of Homogenization Techniques and Conditions on Water-In-Oil Emulsions for Casein Hydrolysate–Loaded Double Emulsions: A Comparative Study, *Food Sci. Nutr.*, 2024, **12**, 9585–9599.
33 E. Chong, H. Abdul Khalil, T. Y. Ying and H. Tajarudin, Preparation and characterization of red seaweed/calcium

carbonate composite films, *IOP Conf. Ser.:Mater. Sci. Eng.*, 2018, **368**, 012041.
34 Z. N. Diyana, R. Jumaidin, M. Z. Selamat and M. S. M. Suan, Thermoplastic starch/beeswax blend: Characterization on thermal mechanical and moisture absorption properties, *Int. J. Biol. Macromol.*, 2021, **190**, 224–232.
35 S. Yoon, S. Chough and H. Park, Properties of starch-based blend films using citric acid as additive. II, *J. Appl. Polym. Sci.*, 2006, **100**, 2554–2560.
36 A. Krishnamurthy and P. Amritkumar, Synthesis and characterization of eco-friendly bioplastic from low-cost plant resources, *SN Appl. Sci.*, 2019, **1**, 1432.
37 A. O. Kaya, A. Suryani, J. Santoso and M. S. Rusli, Characteristic and Microstructure of Mixed Gel of Semi refined carrageenan and Glucomannan, *J. kim. kemasan.*, 2015, **37**, 19.
38 A. H. Dawam Abdullah, B. Firdiana, R. Choerun Nissa, R. Satoto, M. Karina, D. Fransiska, N. Nurhayati, A. Agusman, H. E. Irianto, P. Priambudi, S. Marliah and I. Ismadi, Effect of K-Carrageenan on Mechanical, Thermal and Biodegradable Properties of Starch–Carboxymethyl Cellulose (CMC) Bioplastic, *Cellul. Chem. Technol.*, 2021, **55**, 1109–1117.
39 Z. N. Diyana, R. Jumaidin, M. Z. Selamat, I. Ghazali, N. Julmohammad, N. Huda and R. A. Ilyas, Physical Properties of Thermoplastic Starch Derived from Natural Resources and Its Blends: A Review, *Polymers*, 2021, **13**, 1396.
40 E. Gómez-Ordóñez and P. Rupérez, FTIR-ATR spectroscopy as a tool for polysaccharide identification in edible brown and red seaweeds, *Food Hydrocolloids*, 2011, **25**, 1514–1520.
41 O. J. Gbadeyan, L. Z. Linganiso and N. Deenadayalu, Thermomechanical characterization of bioplastic films produced using a combination of polylactic acid and bionano calcium carbonate, *Sci. Rep.*, 2022, **12**, 15538.
42 Q. Zhang, Y. Li, J. Wen, S. Yuan and Z. Zhu, The effects of CaCO3 on the properties of PCL wood-plastic composites, *IOP Conf. Ser. Earth Environ. Sci.*, 2019, **233**, 022004.
43 S. Abdolmohammadi, S. Siyamak, N. A. Ibrahim, W. M. Z. W. Yunus, M. Z. A. Rahman, S. Azizi and A. Fatehi, Enhancement of Mechanical and Thermal Properties of Polycaprolactone/Chitosan Blend by Calcium Carbonate Nanoparticles, *Int. J. Mol. Sci.*, 2012, **13**, 4508–4522.
44 N. Reddy and Y. Yang, Citric acid cross-linking of starch films, *Food Chem.*, 2010, **118**, 702–711.
45 T. Huhtamäki, X. Tian, J. T. Korhonen and R. H. A. Ras, Surface-wetting characterization using contact-angle measurements, *Nat. Protoc.*, 2018, **13**, 1521–1538.
46 Z. Liu, R. Shen, X. Yang and D. Lin, Characterization of a novel konjac glucomannan film incorporated with Pickering emulsions: Effect of the emulsion particle sizes, *Int. J. Biol. Macromol.*, 2021, **179**, 377–387.
47 L. Cunha and A. Grenha, Sulfated Seaweed Polysaccharides as Multifunctional Materials in Drug Delivery Applications, *Mar. Drugs*, 2016, **14**, 42.
48 Agusman, D. Fransiska, Nurhayati, H. E. Irianto, P. Priambudi, A. H. D. Abdullah, R. C. Nissa, P. P. P. Asri, N. Masruchin, B. B. Sedayu, A. R. Hakim, P. Wullandari and W. T. Handoyo, Effects of Water on Hydrophobization and Mechanical Properties of Thermoplastic Agar, *IOP Conf. Ser. Earth Environ. Sci.*, 2021, **715**, 012057.
49 D. Fransiska, A. H. D. Abdullah, Nurhayati, H. E. Irianto, R. C. Nissa, B. B. Sedayu, F. A. Syamani and S. Raharjo, Suwarti and Agusman, Impact of agar–glycerol ratios on the physicochemical properties of biodegradable seaweed films: A compositional study, *Int. J. Biol. Macromol.*, 2024, **280**, 135855.
50 D. Qiao, W. Tu, L. Zhong, Z. Wang, B. Zhang and F. Jiang, Microstructure and Mechanical/Hydrophilic Features of Agar-Based Films Incorporated with Konjac Glucomannan, *Polymers*, 2019, **11**, 1952.
51 E. Gómez-Ordóñez and P. Rupérez, FTIR-ATR spectroscopy as a tool for polysaccharide identification in edible brown and red seaweeds, *Food Hydrocolloids*, 2011, **25**, 1514–1520.
52 M. A. Chowdhury, N. Hossain, M. D. Badrudduza and M. M. Rana, Development and characterization of natural sourced bioplastic for food packaging applications, *Heliyon*, 2023, **9**, e13538.
53 D. K. Jena and P. K. Sahoo, New strategies for the construction of eggshell powder reinforced starch based fire hazard suppression biomaterials with tailorable thermal, mechanical and oxygen barrier properties, *Int. J. Biol. Macromol.*, 2019, **140**, 496–504.
54 M. Ji, F. Li, J. Li, J. Li, C. Zhang, K. Sun and Z. Guo, Enhanced mechanical properties, water resistance, thermal stability, and biodegradation of the starch-sisal fibre composites with various fillers, *Mater. Des.*, 2021, **198**, 109373.
55 M. C. Meilgaard, B. T. Carr and B. T. Carr, *Sensory Evaluation Techniques*, CRC Press, 2006.
56 *Surface Science Techniques*, ed. G. Bracco and B. Holst, Springer Berlin Heidelberg, Berlin, Heidelberg, 2013, vol. 51.
57 L. Chan, H. M. Nyam, K. L. Yusof and Y. A. Pui, Investigation of Properties of Polysaccharide-Based Edible Film Incorporated With Functional Melastoma Malabathricum Extract, *Carpathian J. Food Sci. Technol.*, 2020, 120–134.
58 A. E. Zeenat, D. A. Bukhari, S. Shamim and A. Rehman, Plastics degradation by microbes: A sustainable approach, *J. King Saud Univ. Sci.*, 2021, **33**, 101538.